January 2013. Vol. 1, No.3 ISSN 2305-8269

International Journal of Engineering and Applied Sciences
© 2012 EAAS & ARF. All rights reserved
www.eaas-journal.org

ANALYSIS OF VERTICAL CAVITY SERFACE EMITTING LASER, RESONANT CAVITY ENHANCED PHOTODETECTOR & THEIR INTEGRATED STRUCTURE

Md. Shamsul Arefin[1]
Tajrian Mollick[2]

[1]Department of EEE, IBAIS University, Dhaka, Bangladesh,
[2]Department of EEE, Bangladesh University, Dhaka, Bangladesh.
arefinshamsul1@yahoo.com

ABSTRACT:

Optoelectronic integrated circuits (OEIC's) are of a tremendous interest because of their high performance characteristics, small size, low cost & expected increased stability. For more efficient OEIC's high performance photo-detectors & LASERs are required. Vertical cavity surface emitting LASERs are the choice for many optoelectronic applications due to their low threshold, single longitudinal mode operation & low beam divergence rather than traditional EELs. As VCSELs have monolithic structure they can be integrated with photo-detectors for to lend themselves in a number of new applications. VCSELs have fabry-perot cavity which has been realized by the distributed bragg reflectors placed on both sides of the cavity region. The resonator structure of VCSEL has made it possible to be with one of the high-speed photo-detector; Resonant Cavity Enhanced Photo-detector, briefly known as RCE-PD. In this photo-detector both high BW & high external quantum efficiency can be achieved simultaneously because of the multi-paths of the incident light due to the presence of the fabry-perot cavity into which the PD is inserted. In this paper the structure, materials requirement & characteristics of the integrated structure of VCSEL & RCE-PD are analyzed. As both of the LASERs & PDs have nearly same structure, there is a good practice to integrate the two structures to increase quantum efficiency to get more bandwidth efficient product. This analysis includes the observation of the quantum efficiency with FWHM, with incident angle & with temperature.

KEYWORDS: *Optoelectronics, EEL, RCE-PD, VCSEL, Quantum Well, Quantum Efficiency.*

I. INTRODUCTION

Modern world cannot think without high speed communication. For this high speed communication VCSEL & RCE-PD are two important optical devices.

1.1 Vertical Cavity Surface Emitting LASER (VCSEL)

Vertical-Cavity Surface-Emitting Lasers (VCSELs) are a relatively recent type of semiconductor lasers. Semiconductor lasers consist of layers of semiconductor material grown on top of each other on a substrate (the "epi"). For VCSELs and edge-emitters, this growth is typically done in a molecular-beam-epitaxy (MBE) or metal-organic-chemical-vapor-deposition (MOCVD) growth reactor. The grown wafer is then processed accordingly to produce individual devices. Figure 1 summarizes the differences between VCSEL and edge-emitter processing.

In a VCSEL, the active layer is sandwiched between two highly reflective mirrors (distributed Bragg reflectors, or DBRs) [1] made up of several quarter-wavelength-thick layers of semiconductors of alternating high and low refractive index. The reflectivity of these mirrors is typically in the range 99.5~99.9%. As a result, the light oscillates perpendicular to the layers and escapes through the top (or bottom) of the device. Current and/or

International Journal of Engineering and Applied Sciences
© 2012 EAAS & ARF. All rights reserved
www.eaas-journal.org

optical confinement is typically achieved through either selective-oxidation of an Aluminum-rich layer, ion-implantation, or even both for certain applications. The VCSELs can be designed for "top-emission" (at the epi/air interface) or "bottom-emission" (through the transparent substrate) in cases where "junction-down" soldering is required for more efficient heat-sinking for example. VCSELs demonstrate excellent dynamic performances such as low threshold currents (a few micro-amps), low noise operation and high-speed digital modulation (10 Gb/s). Furthermore, although VCSELs have been confined to low-power applications – a few mili-Watts at most – they have the inherent potential of producing very high powers by processing large 2-D arrays. In contrast, edge-emitters cannot be processed in 2-D arrays.

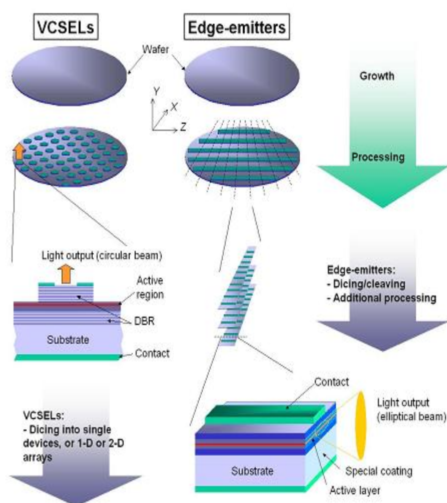

Figure 1. Comparison of the growth/ processing flow of VCSEL & edge-emitter semiconductor lasers.

1.2 Resonant Cavity Enhanced Photo-detector (RCE-PD)

Resonant-cavity-enhanced devices improve efficiency. High-speed RCE photo-detectors offer low cost and high performance for short-distance optical communications and other applications. During the past decade, a new family of optoelectronic devices has emerged with performance that is enhanced by placing the active device structure inside a Fabry-Perot resonant micro-cavity. In such structures, the device functions largely as before but is subject to the effects of the cavity--primarily wavelength selectivity and a large enhancement of the resonant optical field. Optoelectronic devices of this genre are typically referred to as resonant cavity enhanced (RCE). The increased optical field allows photo-detectors to be made thinner and, therefore, faster, while simultaneously increasing the quantum efficiency at the resonant wavelengths. Because off-resonance wavelengths are rejected by the cavity, the photo-detectors exhibit both wavelength selectivity and high-speed response, making them ideal for optical communications. The RCE structure is capable of operating over a large and continuous wavelength range, either by tuning within a material system or by moving to a complementary material system. The superior performance of the RCE photo-detection scheme depends critically on the realization of a low-loss cavity. This requirement dictates that both the mirror and cavity material must be non-absorbing at the detection wavelength and that the mirrors have high reflectivity. The multiple mirror periods, each l/4 thick, have a combined thickness on the order of microns. Therefore, the materials composing the mirror must be well lattice-matched to avoid the introduction of defects into the active layer. To minimize the number of mirror periods-thereby simplifying growth and reducing the device series resistance--it is desirable to have as large a refractive index difference as possible between the mirror materials. The active-layer material must have a smaller band gap than the mirror and cavity materials, but not so much smaller that large hetero-junction-band offsets hinder the extraction of photo generated carriers. The active layer absorption coefficient should be moderate within the operation spectrum to benefit from RCE effect. Various binary and ternary compound semiconductors (such as a GaAs/ (aluminum, indium) GaAs material system) grown by molecular-beam epitaxy allow for band gap engineering in the design of novel RCE structures. The spectrum of RCE photo-detector covers from ultraviolet to infrared with the available semiconductor materials. Figure 2 shows the schematic structure of RCE-PD.

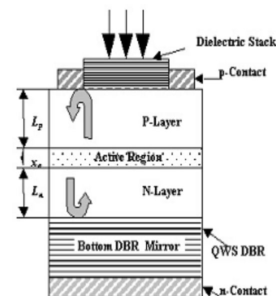

Figure 2. A schematic structure for a RCE-PD.

1.3 Integration of VCSEL & RCE-PD

ISSN 2305-8269

International Journal of Engineering and Applied Sciences
© 2012 EAAS & ARF. All rights reserved
www.eaas-journal.org

VCSEL & RCE-PD can be fabricated on the same device structure. VCSEL is based on the principle is to emit the light where RCE-PD is to absorb the light. The purpose of lasing & photo detection can be served by the same device structure which is the utmost requirement for high speed communication.

1.4 Literature Review

Quantum efficiency is an important figure of merit of photo-detectors. It is the collection efficiency & conversion efficiency combined. It shows how many electron hole pairs are generated per incident photon in a photo-detector. RCE-PD has higher quantum efficiency than other photo-detectors because of its resonant cavity region. Both DC & AC biasing can be used to bias a RCE-PD. VCSEL has the surface emitting property, it is highly efficient for its active region which has Distributed Bragg Reflectors (DBR) on both side. VCSEL is biased by both AC & DC supply. In this paper the quantum efficiency with respect to temperature, incident light angle & top mirror pairs of the integrated structure of RCE-PD with VCSEL is analyzed. The photocurrent & dark current of this integrated structure is also shown. All the measurements are done in reverse bias of -1.5V & zero biasing condition. Implementation of the integrated structure of RCE-PD & VCSEL with AC biasing is recommended at last for future research.

II. MATERIALS & DEVICE STRUCTURE

The top-illuminated VCSEL sample was grown by solid source molecular beam epitaxy (MBE) and contains a half-wavelength-thick inner cavity with three active GaAs quantum wells (QW's) of 8-nm thickness each. The top and bottom mirror consist of 23.5 carbon doped p-type Al0.9Ga0.1As–Al0.2Ga0.8As and 32 silicon doped n-type AlAs–Al0.2Ga0.8As Bragg reflectors, respectively. To achieve lateral current and optical confinement for the VCSEL structures by oxidation, a 30-nm thick Al0.96Ga0.04As–AlAs–Al0.96Ga0.04As layer is placed in the first quarter wavelength layer above the cavity. The schematic of a VCSEL based RCE detector is shown in Figure 3 To form the lateral patterning of the devices a standard VCSEL fabrication process is employed including mesa etching and selective wet oxidation, ring contact deposition, polyimide passivation and bondpad deposition. An additional photolithography step is required for reducing the reflectivity of the p-type top mirror of the RCE devices by etching.

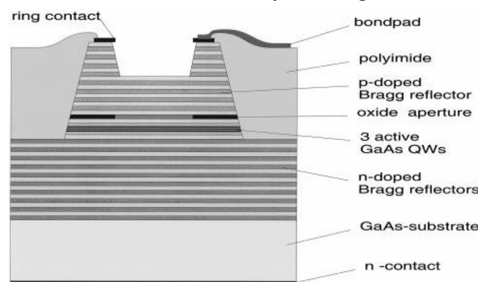

Figure 3. Schematic of a VCSEL based top illuminated RCE detector.

III. RCE DETECTOR MEASUREMENT RESULTS

The quantum efficiency spectrum of RCE devices provides important information about the sensitivity and the wavelength selectivity of the detector. Table 1 & Figure 4 show the influence of a reduced top-mirror reflectivity on the quantum efficiency spectrum of the RCE detector. It is seen that the removal of 8 top-mirror pairs leads to a significant improvement in the quantum efficiency and a slight increase in the FWHM of about 0.2 nm. [2] The etching of 8 top-mirror pairs results in a detector peak quantum efficiency of 73% and 69% with a FWHM of 1.7 and 1.8 nm at a reverse bias of 1.5 V and in the bias-free case, respectively. For a detector with no mirror pairs etched off the peak efficiency is 13% and 11% for -1.5 and 0 V bias voltage, respectively.

Table 1. Spectral quantum efficiency before & after etching of 8 top mirror pairs for 0V & -1.5V.

At -1.5V bias with 8 mirror pairs etched	
Wavelength(nm)	**Quantum Efficiency (%)**
826	1.192
826.8	3.157
827.3	5.448
827.6	7.74
828	14.61
828.5	31.64
828.8	49.97
829	61.1
829.3	68.96
829.8	67.97
830	60.12
830.3	37.86
830.7	18.22
831	12.65
831.5	6.103

International Journal of Engineering and Applied Sciences
© 2012 EAAS & ARF. All rights reserved
www.eaas-journal.org

831.9	4.139
832.5	1.52
833.6	0.865

At 0V bias With 8 mirror pairs etched	
Wavelength(nm)	**Quantum Efficiency (%)**
826.5	2.953
826.7	2.953
827	4.253
827.6	6.203
827.9	10.75
828.5	25.38
828.7	39.35
828.8	43.25
829	51.05
829.7	67.95
830	59.82
830.3	32.85
830.6	20.5
830.7	14.98
831.1	8.153
832.5	1.654
833.1	1.329
833.7	1.004

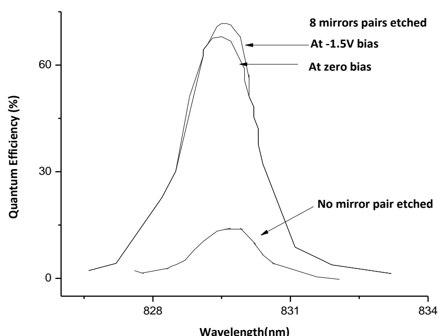

Figure 4. Spectral quantum efficiency before and after etching of 8 top-mirror pairs for 0V and -1.5V bias voltage.

With no mirror pair etched	
Wavelength(nm)	**Quantum Efficiency (%)**
827.6	1.52
828.5	2.174
829	7.412
829.4	10.36
829.6	11.67
830	10.36
830.4	4.793
830.6	3.811
830.9	1.847
831	1.52
831.5	0.865
831.8	1.192
832.2	1.192
832.4	1.192
832.6	1.52
832.9	1.847
833.2	1.847
833.6	0.865

The influence of the top-mirror reflectivity and the applied voltage on the peak quantum efficiency and the related FWHM is summarized in Table 2, Figure 5 and Figure 6 at the detector resonance wavelength. An increase in the FWHM up to 6.5 nm is observed in the spectrum of the 4.5 top-mirror pairs RCE device, for which the quantum efficiency is larger (36%) in the bias-free case. For an applied reverse bias of 1.5 V, the peak efficiency is 26% and is thus smaller for a larger magnitude of reverse bias.

Table 2. Quantum efficiency with top mirror pairs.

At -1.5V bias		At 0V bias	
Top Mirror Pairs	**Quantum Efficiency (%)**	**Top Mirror Pairs**	**Quantum Efficiency (%)**
4.563	37.69	4.563	37.69
4.649	38.03	4.649	38.03
11.72	68.41	11.72	68.41
15.6	69.44	15.6	69.44
17.41	62.61	17.41	62.61
23.1	12.77	23.1	12.77

International Journal of Engineering and Applied Sciences
© 2012 EAAS & ARF. All rights reserved
www.eaas-journal.org

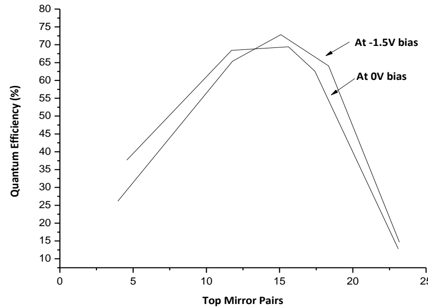

Figure 5. Peak quantum efficiency as a function of top-mirror pairs and applied reverse bias at the detector resonance wavelength.

Table 3. FWHM with top mirror pairs.

At 0V bias		At -1.5V bias	
Top Mirror Pairs	**FWHM nm**	**Top Mirror Pairs**	**FWHM nm**
3.959	6.287	3.959	6.287
4.132	6.198	4.132	6.198
7.752	4.519	7.752	4.519
8.442	4.165	8.442	4.165
8.528	4.135	8.528	4.135
9.735	3.575	9.735	3.575
14.56	1.218	14.56	1.218
15.08	1.011	15.08	1.011
15.25	0.9819	15.25	0.9819
17.23	0.805	17.23	0.805
17.75	0.805	17.75	0.805
19.99	0.7166	19.99	0.7166
20.85	0.6577	20.85	0.6577
21.37	0.6282	21.37	0.6282
21.98	0.5987	21.98	0.5987
22.58	0.5693	22.58	0.5693
23.18	0.5398	23.18	0.5398

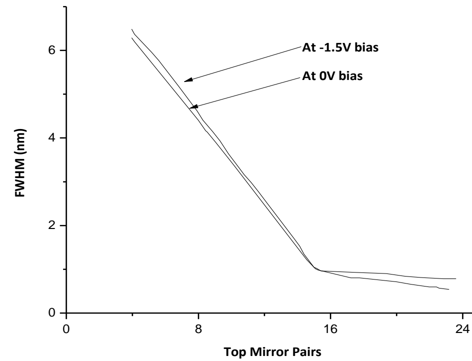

Figure 6. FWHM as a function of top-mirror pairs and applied reverse bias at the detector resonance wavelength.

Table 4 & Figure 7 show the angle dependent quantum efficiency where the constant incident wavelength matches the detector resonance wavelength at normal incidence. The decrease is about 3% for an angle of 3° and about 8% for an angle of 5°. Such angular dependence to the detector performance shows that one need not expect significant angular alignment difficulties for RCE detectors using small numerical aperture optics.

Table 4. Quantum Efficiency with incident light angle at 0V & -1.5V.

At -1.5V bias		At zero bias	
Incident Light Angle (Degree)	**Incident Light Angle (Degree)**	**Incident Light Angle (Degree)**	**FWHM nm**
0.4585	0.5171	0.5171	6.287
1.738	0.7487	0.7487	6.198
2.261	3.296	3.296	4.519
2.784	4.164	4.164	4.165
3.889	5.496	5.496	4.135
4.587	6.248	6.248	3.575
5.808	6.885	6.885	1.218
6.215	7.464	7.464	1.011
7.494	7.869	7.869	0.9819

International Journal of Engineering and Applied Sciences
© 2012 EAAS & ARF. All rights reserved
www.eaas-journal.org

8.192	8.854	8.854	0.805
8.948	9.896	9.896	0.805
9.413	10.42	10.42	0.7166
9.936	11.34	11.34	0.6577
10.87	11.86	11.86	0.6282
11.97	12.44	12.44	0.5987
12.96	12.73	12.73	0.5693

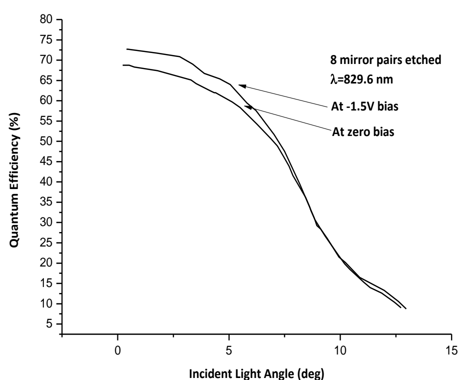

Figure 7. Measured quantum efficiency with respect to the incident light angle at 0V and -1.5V bias voltage.

The thermal behavior of the quantum efficiency is shown in Figure 8, Table 5 & Table 6. The constant incident wavelength matches the detector resonance wavelength at room temperature. The measurement reveals that the efficiency decay is more than twice as high for temperatures below room temperature as for temperatures above. This behavior is most likely related to an increasing QW absorption coefficient with temperature.

Table 5. Quantum Efficiency at different devices temperatures for -1.5V.

At -1.5V bias	
Temperature(˚C)	**Quantum Efficiency (%)**
5.964	53.55
7.706	61.17
11.19	68.12
18.66	71.94
20.52	70.59
26.5	69.25
29.98	66.56
31.85	63.19
35.83	60.5
38.82	54.67
40.44	48.62
44.29	39.65
49.89	29.79
53.5	25.98
55	23.74
55.24	23.96

Table 6. Quantum Efficiency at different devices temperatures for 0V.

At 0V bias	
Temperature(˚C)	**Temperature(˚C)**
4.869	4.869
8.967	8.967
14.74	14.74
18.65	18.65
27.78	27.78
29.27	29.27
32.25	32.25
34.86	34.86
35.04	35.04
36.53	36.53
38.95	38.95
41.93	41.93
44.35	44.35
48.64	48.64
49.76	49.76
55.34	55.34

International Journal of Engineering and Applied Sciences
© 2012 EAAS & ARF. All rights reserved
www.eaas-journal.org

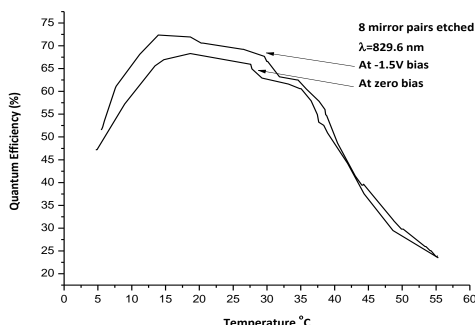

Figure 8. Measured quantum efficiency at different device temperatures for 0V and -1.5V bias voltage.

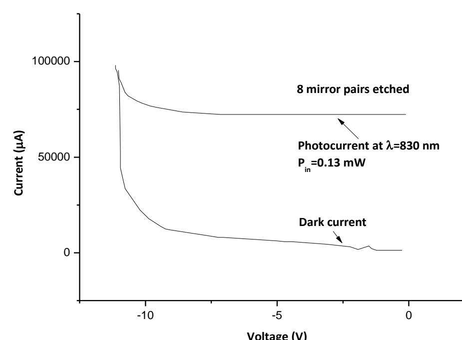

Figure 9. Measured photocurrent with respect to the incident light power for the 8 top-mirror periods etched device.

To exclude saturation effects the photocurrent with respect to the incident light power of the 8 top-mirror pairs etched device has been measured. The photocurrent shows a linear dependence up to the maximum incident power delivered by the setup of 3.8 mW. The related maximum current was 1.8 mA. This confirms that saturation effects play no role in the measurements, since the power used for the characterization was kept below 1 mW. From RCE detector dark current measurements in Figure 9 & Table 7, a maximum value of -100 pA at -10 V is obtained and the breakdown voltage is -10.8 V. Thus, the dark current is about six orders of magnitude lower than common RCE detector photocurrents in the range of 10 to 100 A.

Table 7. Photocurrent with respect to incident light power for the 8 top mirror pairs etched.

Photocurrent		Dark current	
Voltage (V)	Current (μA)	Voltage (V)	Current (μA)
-11.03	95540	-11.14	98140
-11	91080	-10.21	22370
-10.92	88850	-9.245	12500
-10.78	83930	-9.097	12060
-10.67	82150	-7.425	8470
-10.33	79470	-7.239	8021
-10.11	78130	-7.054	8021
-9.817	76790	-5.011	6228
-9.522	75900	-4.713	5780
-9.337	75450	-3.079	4435
-8.599	73660	-2.224	3090
-7.16	72330	-1.407	2193
-0.1119	72330	-0.2557	1296

IV. DISCUSSION

In this paper the basic structures, characteristics, material requirements of VCSELs have been discussed in details. VCSELs are updated and advantageous over the EEL (Edge Emitting Laser). Much higher power can be generated with VCSEL [3]. The processing cost is lower than EEL because of having the opportunity to test each part or layer after growth. After the analysis it is clear that VCSEL is very stable to sense the wavelength, temperature dependency is lower, per unit area power generation is high, its beam quality increases the coupling efficiency, reliability is high over others laser. In a word, VCSEL is very much effective to do further research to improve the laser power capability. VCSEL structure can be used as the photo-detector doing a small modification. It is an advantage to use the same structure as both laser and photo-detector. VCSEL is very much usable in advanced applications in the field of laser operation. Now-a-days VCSEL is used largely in the optical communications.

The main purpose of this paper is to analysis the VCSEL applications and the structure similarity between the basic VCSEL and the RCE-PD to use the same structure in both purposes. The structure of the VCSEL can be used as both the laser and RCE-PD with a modulation changing the direction of biasing. This will reduce the cost and space where both applications are applied simultaneously. This characteristic of the structure has been shown in this paper using the ORIGIN and FINDGRAPH software.

ISSN 2305-8269

International Journal of Engineering and Applied Sciences
© 2012 EAAS & ARF. All rights reserved
www.eaas-journal.org

V. CONCLUSION

This paper is based on the analysis of the integration of VCSEL & RCE-PD. DC biasing is used here. The individual structure of VCSELs [3] & RCE-PDs [2] was biased with AC supply. The integrated structure of VCSEL & RCE-PD can be biased with AC voltage, and then there must be filtration facility to implement. AC biasing must require definite discussion about the carrier conditions of both the LASER & PD. In this paper only AlGaAs & GaAs materials are used for the integrated structure. InGaAs & InGaAsP, InP should be used to implement this type of device structure for better performance.

VI. ACKNOWLEDGEMENT

There are many people who have supported and encouraged us during our works. This has meant a lot of us and we are very grateful to all of them. We would like to take this opportunity to especially acknowledge the following people for their various contributions to this work. Dr. Mohammad Jahangir Alam, Professor, Department of Electrical & Electronic Engineering, BUET was of great support for us throughout the work. We also acknowledge that without his continuous guidance, enthusiasm, encouragement and valuable suggestion this thesis work would not have been possible. We are indebted to him for his modern outlook and cordial supervision. Last but not the least, we thank to the Almighty Allah to bring this work into reality.

VII. REFERENCES

[1] J.P. Van Der Ziel and M. Ilegems, "Multilayer GaAs-Al0.3Ga0.7As dielectric quarter wave stacks grown by molecular beam epitaxy", Applied Optics, 14, pp. 2627-2630, 1975.

[2] Yasser M. El-Batawy and M. Jamal Deen, "Resonant Cavity Enhanced Photo-detectors (RCE-PDs): Structure, Material, Analysis and Optimization," Proceedings of SPIE, Vol 4999, pp. 363-378, 2003

[3] Jim Tatum, David Smith, Jim Guenter and Ralph Johnson, "High Speed Characteristics of VCSELs".